

Hip Fracture Prediction using the First Principal Component Derived from FEA-Computed Fracture Loads

Xuewei Cao^{1,#}, Joyce Keyak^{2,#}, Sigurdur Sigurdsson³, Chen Zhao⁴, Weihua Zhou⁴, Anqi Liu⁵, Thomas Lang⁶, Hong-Wen Deng⁵, Vilmundur Gudnason^{3,7,*}, Qiuying Sha^{1,*}

¹ Department of Mathematical Sciences, Michigan Technological University, Houghton, Michigan, USA

² Department of Radiological Sciences, Department of Biomedical Engineering, and Department of Mechanical and Aerospace Engineering, University of California, Irvine, CA, USA

³ Icelandic Heart Association Research Institute, Kópavogur, Iceland

⁴ Department of Applied Computing, Michigan Technological University, Houghton, MI, USA

⁵ Center for Bioinformatics and Genomics, School of Medicine, Tulane University, New Orleans, LA, USA

⁶ Department of Radiology and Biomedical Imaging, University of California, San Francisco, CA, USA

⁷ University of Iceland, Reykjavik, Iceland

Both authors contributed equally

* Corresponding authors: Qiuying Sha, Department of Mathematical Sciences, Michigan Technological University, Houghton, Michigan 49931, USA. E-mail: qsha@mtu.edu

Vilmundur Gudnason, Icelandic Heart Association Research Institute, Kópavogur, Iceland. E-mail: v.gudnason@hjarta.is

Abstract

Hip fracture risk assessment is an important but challenging task. Quantitative CT-based patient-specific finite element analysis (FEA) incorporates bone geometry and the three-dimensional distribution of bone density in the proximal femur to compute the force (fracture load) and energy necessary to break the proximal femur in a particular loading condition. Although the fracture loads and energies for different loading conditions are individually associated with incident hip fracture, and are mutually correlated, they each provide different structural information about the proximal femur that can influence a subject's overall fracture risk. To obtain a more robust measure of fracture risk, we used principal component analysis (PCA) to develop a global FEA-computed fracture risk index that incorporates the FEA-computed yield and ultimate failure loads and energies to failure in four loading conditions (single-limb stance and impact from a fall onto the posterior, posterolateral, and lateral aspects of the greater trochanter) of 110 hip fracture subjects and 235 age- and sex-matched control subjects from the AGES-Reykjavik study. We found that the first PC (PC1) of the FE parameters was the only significant predictor of hip fracture ($p<0.001$); we refer to PC1 as the global FEA-computed fracture risk index. To evaluate this fracture risk index, we considered seven covariates including demographic and clinical parameters. Using a logistic regression model, we determined if prediction performance for hip fracture using PC1 differed from that using FE parameters combined by stratified random resampling with respect to hip fracture status. We also compared the performance of predicting hip fracture using the logistic regression model with PC1 and the FRAX model. The results showed that the average of the area under the receive operating characteristic curve (AUC) using PC1 (0.776) was always higher than that using all FE parameters combined (0.737) in the male subjects ($p<0.001$). The AUC of PC1 and AUC of the FE parameters combined were not significantly different than that in the female subjects ($p=0.211$) or in all subjects ($p=0.159$). The AUC values using PC1 (0.754 in all subjects, 0.825 in males and 0.71 in females) were greater than those using FRAX (0.651 in the whole sample, 0.705 in male and 0.623 in female) with $p<0.01$. Therefore, the global FEA-computed fracture risk index based on PCA includes information about hip fracture incidence beyond that of FRAX.

Introduction

Osteoporosis is among the most common and costly metabolic bone diseases [1], in which the density and quality of bone are reduced. It is characterized by excessive skeletal fragility and susceptibility to low-trauma fracture among the elderly [2-4], causing bones to become weak and brittle and greatly increasing the risk of fracture [5,6]. The incidence and prevalence of osteoporosis increases with age and is related to many factors, such as gender, weight, height, and medical/medication history [7,8]. The increasingly elderly population and the rise in fracture incidence have made osteoporosis a major public health issue in the U.S. and around the world. Osteoporosis affects about 25% of women aged \geq 65 and about 5% of men aged \geq 65 [9]. The economic burden of osteoporosis has been estimated at between \$17 billion and \$20.3 billion in the US alone (2020 data) [10].

Although osteoporosis can affect any bone in the human body, osteoporotic fractures of the proximal femur are the most devastating outcome of the disease, often signaling an end to independent living in the functional elderly. Each year over 300,000 older people in the U.S.—many of those 65 and older—are hospitalized for hip fracture. 5-10% of patients experience a recurrent hip fracture [11]. Hip fractures are invariably associated with chronic pain, reduced mobility, disability, and an increasing degree of dependence [12]. Hip fractures cause the most morbidity; reported mortality rates are up to 20-24% in the first year after a hip fracture [13,14], and a greater risk of dying may persist for at least 5 years afterwards [15]. Loss of function and independence among survivors is profound; 40% are unable to walk independently and 60% require assistance a year later [16]. Because of these losses, 33% are totally dependent or in a nursing home in the year following a hip fracture [17,18]. Less than half of those who survive the hip fracture regain their previous level of function [12]. Fracture risk assessment and risk stratification through screening are necessary to reduce the incidence of hip fracture.

Areal bone mineral density (aBMD) of the proximal femur assessed by dual energy X-ray absorptiometry (DXA) is the accepted clinical parameter for the diagnosis of osteoporosis of the hip [19-21]. The aBMD is compared with that of a reference group to obtain the number of standard deviations from the mean aBMD of a gender- and ethnicity-

matched healthy population, i.e., the T-score [22,23]. Although low DXA aBMD is associated with bone weakness and fragility fracture [24], DXA is a 2D-projection technique that poorly accounts for bone geometry and size, and it cannot separately evaluate the cortical and trabecular bone [25]; all of these factors influence the integrity of the proximal femur and, therefore, the risk of fracture. Thus, DXA aBMD provides limited information about skeletal factors on fracture risk.

Quantitative CT (QCT) imaging is one of the most powerful methods for assessing bone quality in the proximal femur; after three-dimensional (3D) segmentation of the proximal femur, features such as volumetric bone mineral density (BMD) of the cortical and trabecular bone and bone geometry can be computed. Therefore, QCT is better than DXA for evaluating fracture risk [26]. Patient-specific finite element analysis (FEA) from QCT images incorporates bone geometry, cortical thickness, and the three-dimensional distribution of bone density in the proximal femur to compute the force (fracture load) necessary to break the proximal femur in a particular loading condition. The fracture load can be defined as the force at the onset of fracture (the yield strength) or the maximum force the proximal femur withstands before complete fracture (the ultimate strength or load capacity), and are calculated using FEA with linear or nonlinear material properties, respectively. FEA-computed fracture loads are the most robust measure of proximal femoral structural integrity and, therefore, hip fracture risk [27,28]. In particular, the ultimate strength or load capacity of the proximal femur which is computed with nonlinear FEA is associated with incident hip fracture in men and women, and in men even after controlling for aBMD [8].

Finite element models compute the force necessary to break the proximal femur when forces and other boundary conditions are applied to reflect a specific loading condition, such as single-limb stance during walking or impact onto the greater trochanter from a fall in a specific direction [8]. Although the FEA-computed yield or ultimate strengths for different loading conditions are individually associated with incident hip fracture, and are mutually correlated, the yield and ultimate strength for each loading condition each provide different structural information about the proximal femur that contribute to a subject's overall hip fracture risk. The energy transferred to the proximal

femur prior to reaching ultimate failure in particular loading conditions may also be associated with fracture risk. Therefore, in this study we examined a combination of the FEA-computed yield and ultimate strengths and energies-to-failure in various loading conditions to obtain a more robust measure of fracture risk than individual FEA-computed strengths. Principal component analysis (PCA) is a commonly used method to reduce the dimensionality of the data by selecting the most important features that capture the most information [29]. PCA can also speed up the algorithm for prediction by getting rid of correlated variables which do not contribute to decision making [30]. Therefore, we employed PCA to develop a global FEA-computed hip fracture risk index based on the FE model results of 110 hip fracture subjects and 235 age- and sex- matched control subjects in a subset of the AGES-Reykjavik study [31]. PCA is one of the most widely used dimension reduction techniques to transform the larger number of variables into a smaller number of variables by identifying the correlations and patterns, while preserving most of the valuable information. The objectives were (1) to construct a global FEA-computed risk index based on PCA that is associated with incident hip fracture; (2) to determine if the global FEA-computed risk index, after adjusting for covariates, predicts hip fracture better than the FE yield, ultimate strengths and energies-to-failure combined; (3) to compare the predictive performance of the global FEA-computed risk index with FRAX with covariates.

Methods

Subjects

In this study, we used 110 hip fracture subjects and 235 age- and sex matched control subjects from the Age Gene/Environment Susceptibility (AGES) Reykjavik study [8,31]. The AGES-Reykjavik study is an ongoing population-based study which contains the baseline QCT scans of subjects who had no metal implants at the level of the hip [31]. Subjects were followed for 4 to 7 years (y), through November 15, 2009. Forty-two males and 68 females suffered hip fractures during the follow-up period. Meanwhile, 92 male and 143 female control subjects were selected from a pool of age- and sex-matched subjects. The age of the male fracture group was from 71 y to 93 y with the standard deviation (SD=5.6 y), and that of the female fracture was from 67 y to 93 y with SD=5.9 y

(Table 1). Accordingly, the age range of the control male was from 70 y to 90 y with SD=5.2 y and that of the control female was from 67 y to 92 y with SD=5.7 y. The average heights were 174.6 cm and 174.9 cm for fracture male and control male, respectively. The average heights were 159.6 cm and 159.2 cm for fracture female and control female, respectively.

FEA-computed parameters

The FE models simulated mechanical testing of the femur in which displacement was incrementally applied to the femoral head. The computed reaction force on the femoral head initially increased, reached a peak value (the fracture load), and then decreased. To achieve this mechanical behavior, the FE models employed heterogeneous isotropic elastic moduli, yield strengths, and nonlinear post-yield properties. These properties were computed from the calibrated QCT density (ρ_{CHA} , g/cm³) of each voxel in an element, which was then used to compute the ash density (ρ_{ash} , g/cm³) ($\rho_{ash} = 0.0633 + 0.887 \rho_{CHA}$), and ρ_{ash} was used to compute mechanical properties. Each linear hexahedral finite element measured 3 mm on a side and the mechanical properties of the element were computed by averaging the values of each property over all voxels in the element, while accounting for the volume fraction of each voxel within the element. Together, these mechanical properties described an idealized density-dependent nonlinear stress-strain curve for each element [8,32]. Material yield was defined to occur when the von Mises stress exceeded the yield strength of the element. After yield, the plastic flow was modeled assuming a plastic strain-rate vector normal to the von Mises yield surface and isotropic hardening/softening. Displacement was applied incrementally to the femoral head, and the reaction force on the femoral head was computed at each increment as the distal end of the model was fully constrained. For the fall models, the surface of the greater trochanter opposite the loaded surface of the femoral head was constrained in the direction of the displacements while allowing motion transversely. The FE-computed hip fracture load was defined as the maximum FE-computed force on the femoral head.

Based on our FE modeling method from the QCT data [33-36], twelve FE parameters were evaluated for each subject: yield strength, ultimate failure load, and

energy-to-failure calculated single-limb stance and impact from a fall onto the posterior, posterolateral, and lateral aspects of the greater trochanter (refer to Table 2 to define the variable abbreviations). The yield strength was defined as the load at which the von Mises stress in 15 contiguous finite elements exceeded the yield strength for the element. Ultimate strength was defined the maximum reaction force on the femoral head. Energy-to-failure was defined as the area under the force versus displacement curve up to the ultimate strength. The Pearson correlation coefficient was applied to measure the linear correlation among 12 FE parameters. Although fracture parameters were inherently correlated, the fracture load for each loading condition provided different structural information about the proximal femur that contributes to a subject's overall fracture risk.

Statistical analysis

To identify which FE parameters were the most important determinants of fracture risk, the data for male and female subjects were analyzed together in a single model and multiple regression analysis was performed with each FE parameter serving as the dependent variable [8]. Thus, the *p*-value indicated the evidence of the association between FE parameter and fracture status (FX; yes or no), and the coefficient of determination (R^2) indicated the proportion of the variability in the FE parameter that was accounted for by the regression model. Based on our previous study [8], fracture status and demographic parameters, age, sex, height, and weight were considered as candidate independent variables. Interactions between fracture status and the demographic parameters were also considered. We started with a simple linear regression model to test the association between each of the candidate independent variables and each of the 12 FE parameters. In the multiple linear regression, we only retained the variables with $p < 0.1$. Also, if an interaction term was retained, the individual variables making up that interaction were retained, regardless of the *p*-value for the individual variable. The multiple linear regression analyses were performed for each of the FE parameters accounting for the retained independent variables. In all of these analyses, FE parameters, age, height, and weight were standardized by subtracting the mean and dividing by the SD of the pooled data.

Principal component analysis and Hip fracture prediction

The FE parameters for each loading condition provided different structural information about the proximal femur that contribute to a subject's overall fracture risk. Therefore, to obtain a more robust measure of fracture risk, we investigated principal component analysis (PCA) to develop a global FEA-computed risk index based on the FE parameters which were mutually correlated. Instead of analyzing data from males and females combined (all sample), we also applied PCA to the male sample and female sample, separately. We used a logistic regression model to test the association between the hip fracture status and each of the principal components. Let FX be the fracture status, where $FX = 1$ if the subject suffered a hip fracture and $FX = 0$ otherwise. For the j^{th} principal component, the logistic regression model was expressed by $\text{logit}(\text{Pr}(FX)) = \beta_{0j} + \beta_{1j}PC_j$. The top principal components were retained with $p < 0.05$. To compare the hip fracture prediction performance using the global FEA-computed fracture risk index, we considered seven covariates which contain four demographic parameters, age, sex, height, and weight, and three clinical parameters, health status (HEALSTAT; excellent, very good, good, fair, or poor), bone medication status (BMDMED; yes or no), and CT-derived total femur areal bone mineral density (BMD) which has a strong correlation with areal BMD from DXA ($r = 0.935$) [27]. The area under the receiver operating characteristic (ROC) curve (AUC) indicates the predictive performance for each of the classification models. We divided the data based on the incidence of hip fracture into a training set (80% of subjects) and test set (20% of subjects) and analyzed male subjects separately from female subjects as well as analyzing the whole sample. To choose the best predictive model based on the training set, we used three linear classification models, including logistic regression (Logistic), linear discriminant analysis (LDA), and partial least squares analysis (PLS), along with six nonlinear classification models, random forest (RF), quadratic discriminant analysis (QDA), mixture discriminant analysis (MDA), neural networks (NNET), multivariate adaptive regression splines (MARS), and K-nearest neighbors (KNN) [37]. Using the training set, we investigated stratified leave-one-group-out cross-validations (LGOCVs), repeating this procedure 25 times. For each LGOCV, we used 75% of the data to build the classification models and 25% of the data to predict and calculate the AUC. After choosing the best models, we trained those models using the entire training set and predicted the fracture status based on the test set. To compare

the performance for predicting hip fracture using (a) the global FEA-computed fracture risk index with the covariates, (b) the FE parameters with the covariates, and (c) the covariates only, we performed stratified resampling 1000 times and applied a one-sided Student's t-test that compared the resampled AUCs.

Comparison with FRAX

The fracture risk assessment (FRAX) tool (<https://www.sheffield.ac.uk/FRAX/>), released in 2008 by the University of Sheffield, computes individualized 10-year probability of osteoporotic fracture and hip fracture risk [38]. Age, sex, weight, height, previous fracture, parent fractured hip, smoking status, use of oral glucocorticoids, rheumatoid arthritis, and secondary osteoporosis, and alcohol intake of subjects from Iceland study were entered into the FRAX calculator. In the previous study comparing CT-derived areal BMD with actual areal BMD from DXA (Lunar Prodigy, GE Medical Systems, Milwaukee, WI), a strong linear relationship between these two measures was reported (DXA areal BMD (g/cm²) = 0.924*CT-derived areal BMD (g/cm²) + 0.137; $r = 0.935$; standard error of the estimate (SEE) = 0.046 (g/cm²)) [27]. Therefore, we used this relationship to correct the CT-derived areal BMD to obtain DXA-equivalent areal BMD, then entered the corrected values, DXA total femur areal BMD for the Lunar Prodigy, into FRAX. We used one-sided DeLong's test if two ROC curves were significantly different.

Results

The descriptive statistics for subjects (i.e., median, average, range, etc.) were listed in Table 1. Within the male sample, the fracture and control groups were not significantly different with respect to age, height, weight, and three energy-to-failure loading conditions (PLenergy, Penergy, Lenergy) at the time of the CT scan ($p>0.120$; Table 1). However, the remaining eight FE parameters were significantly lower in each fracture group than in the respective control group ($p<0.001$). In contrast, within the female sample, the fracture and control groups were significantly different with respect to weight ($p=0.036$). Age, height, and the same three energy-to-failure loading conditions were not significantly different between fracture and control groups ($p>0.513$). Similarly, the remaining eight FE parameters were also significantly lower in each fracture group

than in the respective control group (nonlinear lateral strength, $p=0.007$; all others, $p<0.001$).

Multiple linear regression analyses were performed for each of the FE parameters accounting for the retained independent variables and interactions (Table 3). Even though we controlled for demographic variables and interactions, linear regression revealed that the FE parameters were associated with hip fracture with $p<0.1$, except for Pu, PLenergy, Penergy, and Lenergy. Therefore, we only considered eight hip fracture-related FE parameters along with Pu ($R^2 = 0.5217$) in the following analysis. The PCA was applied to these nine FE parameters, which were inherently highly correlated (Figure 1). The proportions of variance explained by the first PC (PC1) are 83.31%, 78.23%, and 80.65% for all sample, male sample, and female sample, respectively. We found that the PC1 of the FE parameters was the only significant predictor for hip fracture ($p<0.001$ in all sample, male sample, and female sample), therefore, we referred to PC1 as the global FEA computed fracture risk index. Using the LGOCV, we found that the performance of using PC1 and covariates, or the nine FE parameters combined and covariates, were better than that of only using covariates to predict hip fracture (Table 4). In particular, we observed the superior predictive performance within all sample and male sample of PC1 compared with FE parameters combined for all nine classification models; while, within the female sample, FE parameters combined had larger AUCs than PC1. Logistic and PLS had the largest AUCs among nine models (Table 4), which were chose as two best models. The predictive performance of PLS and Logistic based on stratified resampling were shown in Figure 2 and Figure 3. For all sample, Logistic performed better than the PLS by using PC1 and FE parameters combined along with the covariates, which were also better than Logistic using only covariates ($p<0.001$). In contrast, within the male sample, PLS using PC1 and FE parameters combines along with the covariates were better than PLS using only covariates ($p<0.001$). In particular, we observed the superior predictive performance in male sample of PC1 compared with each FE parameter based on PLS ($p=0.02$ for Ly; all others, $p<0.01$) (Figure 3). For the female sample, all of the AUCs of PLS using one of the FE parameters were greater than the corresponding AUC using PC1 with $p>0.1$, except for Ly ($p=0.0145$).

Finally, to compare the performance of the hip fracture prediction between PC1 and FRAX, we used the logistic regression model adding the information of PC1 along with seven covariates for three cohorts (whole, male, female). The corrected CT-derived areal BMD are ranging from 0.137 (g/cm²) to 1.148 (g/cm²) (mean±SD: 0.597±0.118 (g/cm²)). Figure 4 showed that the AUC using PC1 (0.754 in all sample, 0.825 in male and 0.71 in female) was greater than that using FRAX (0.651 in the whole sample, 0.705 in male and 0.623 in female). The global FEA computed fracture risk index based on PCA includes information about hip fracture incidence beyond that of FRAX ($p<0.01$) (Figure 4).

Discussion

This is the first study to construct a global FEA-computed risk index that is investigated by principal component analysis based on multiple fracture-related FEA-computed fracture loads and energies under different loading conditions. The global FEA-computed risk index, after adjusting for covariates, predicted hip fracture better than the individual FE yield, ultimate strengths and energies-to-failure and combined within all sample and male sample (Figures 2-3, Table 4). However, within the female sample, the FE parameters combined better than the global risk index but no differences than each of FE parameters except for Ly ($p=0.0145$) (Figures 2-3, Table 4). These differences between the predictive performance in men and women implied that the sex differences in FE parameters largely stem from the original QCT density data. Meanwhile, predicting fracture in the female sample was inherently more difficult than predicting fracture in the male sample because the difference between female fracture and control subjects is much smaller than that for males. Same as our previous work [8], the age-matched design of this study enhanced our ability to explore gender differences in proximal femoral strength and incident hip fracture as a function of age. In particular, our cross-sectional analysis of age-related FE loads less by gender and fracture status may explain why proximal femoral strength was strongly associated with incident hip fracture in men but much less so in women.

Although the FE parameters were individually associated with incident hip fracture, and were mutually highly correlated (Figure 1), they each provided different structural

information about the proximal femur that can influence a subject's overall fracture risk. The superior performance, in both men and women, of the assessment of hip fracture risk by using the global FEA-computed risk index and FE parameters combined along with covariates compared with only covariates is not surprising. The CT-derived total femur areal BMD was considered as one of the covariates, which has a strong correlation with areal BMD from DXA ($r = 0.935$) [27]. The predictive performance by incorporating information from FE parameters were better than only using covariates in the male sample and female sample (Figure 2, Table 4), implying that the FE parameters can provided additional information in the assessment of hip fracture risk by incorporating bone geometry, cortical thickness, and the three-dimensional distribution of bone density in the proximal femur. Meanwhile, the global FEA-computed risk index plus the areal BMD from DXA was better than the areal BMD only (Figure 2, Table 4). Although areal BMD from DXA correlated with bone weakness and fragility fracture [24], DXA is a 2D-projection technique that poorly accounted for bone geometry and size and is a poor predictor of hip fracture in subjects with osteopenia (T-scores between -1 and -2.5). Thus, areal BMD provides limited information about skeletal factors on fracture risk. However, with the emergence of QCT scan-based FE modeling, better estimates of proximal femoral strength have become possible [39]. Our study employed three-dimensional (3-D) FE models from QCT scans, which explicitly represented the 3-D geometry and distribution of material properties that made each femur structurally and mechanically unique and were therefore considered more robust than two-dimensional (2-D) models from DXA. Principles of physics dictate that hip fracture occurs when an excessive force is applied to the proximal femur, i.e., when the applied force exceeds the force that the proximal femur can support. This force, which varies with the type of loading and force direction, is known as the proximal femoral strength, fracture load [8,34], or load capacity [32] and was computed using patient-specific finite element (FE) analysis (FEA). Patient-specific FEA-computed fracture loads and energies were the most robust measures of proximal femoral structural integrity and, therefore, benefitted for evaluating the hip fracture risk.

Further, this global risk index improved assessment of hip fracture risk beyond the commonly used method for evaluating hip fracture risk, namely FRAX (Figure 4), using

all sample, the male sample, and the female sample. The FRAX model estimated the 10-year probability of hip fracture, which failed to capture all skeletal determinants of bone strength that tend to be independent of BMD [40,41]. As FRAX only included BMD from DXA as an input, it may be clinically more appropriate to use the FE parameter from QCT scans in assessing the hip fracture risk of subjects. Although our study has a number of important advantages, such as the age- and sex- matched case-control prospective design and analysis multiple fall loading conditions, the AUC for FRAX of the AGE-Reykjavik cohort was calculated based on the incidence of hip fracture using the estimated 10-year probabilities of hip fracture. Our method was evaluated using the fractures that occurred over 4 to 7 years, which became a limitation to compared with 10-year probabilities of hip fracture from FRAX. However, this study has important clinical implications for the use of 3-D FE models to improving assessment of hip fracture risk, particularly in the high-risk cohort of elderly subjects admitted to hospital following falls. This study identified the clear need for flexibility in using appropriate risk calculators to improve healthcare delivery.

Conclusions

In summary, FEA-computed fracture loads and energies were associated with incident hip fracture in most of loading conditions that were examined, and the global FEA-computed risk index that was investigated by principal component analysis in the male sample increased hip fracture risk prediction accuracy more than that in the female sample. The global FEA-computed risk index was most strongly associated with incident hip fracture in men after accounting for areal BMD from DXA and other clinical and demographic parameters. Thus, FE parameters from 3-D FE models includes information about hip fracture beyond that of areal BMD from 2-D models and that of FRAX, especially in the male sample. The significance and complexity of these findings, particularly with respect to sex and age effects, indicate that additional studies of FE modeling for hip fracture risk assessment are likely to enhance our understanding of this significant public health problem.

CONFLICT OF INTERESTS

The authors declare that there is no conflict of interests.

ACKNOWLEDGMENTS

This study was supported by NIH/NIA R01AG028832 and NIH/NIAMS R01AR46197. The Age, Gene/Environment Susceptibility Reykjavik Study is funded by NIH contract N01-AG-12100, the NIA Intramural Research Program, Hjartavernd (the Icelandic Heart Association), and the Althingi (the Icelandic Parliament). The study was approved by the Icelandic National Bioethics Committee, (VSN: 00-063) and the Data Protection Authority. The researchers are indebted to the participants for their willingness to participate in the study. HWD was partially supported by U19 AG055373 and R01 AR069055. XC was funded by the Michigan Technological University Health Research Institute Fellowship program and the Portage Health Foundation Graduate Assistantship.

Table 1. Descriptive statistics for subjects with incident hip fracture and the age- and sex-matched controls. Statistical significance of differences between cases and controls was established using Student's t-test

Sex	Measure	Controls					Cases					p		
		N	Min	Max	Median	Average	SD	N	Min	Max	Median	Average		
Male	AGE	92	70	90	80	79.7	5.2	42	71	93	81	80.5	5.8	0.432
	HEIGHT	92	162.4	190.5	174.2	175	6.6	42	159.2	187.1	174	174.9	5.4	0.941
	WEIGHT	92	52.4	135	82	82.8	14.9	42	50.3	111.3	77.5	78.7	13.5	0.120
	PLy	92	638	4257	1626	1704	673.9	42	276	2254	1202.5	1202.4	465.1	<0.001
	PLu	92	2408	5499	3733.5	3838.6	570.2	42	1723	4269	3253.5	3311.1	529.5	<0.001
	Sy	92	2043	13990	4697.5	5010.5	1912.5	42	1261	6824	3380.5	3524.4	1219.2	<0.001
	Su	92	4772	21784	9992.5	10628.1	2967.8	42	3123	12898	7980.5	7980.2	2017.2	<0.001
	Py	92	631	4123	1699	1821.3	655.7	42	404	2014	1295	1294.6	415.9	<0.001
	Pu	92	2149	5078	3322	3322.9	456.1	42	1766	3964	3013	2954.9	426.3	<0.001
	Ly	92	1028	5393	2063	2141.5	745.3	42	441	2957	1427	1476.1	507.8	<0.001
	Lu	92	2344	6619	4299.5	4315.2	743.9	42	1913	4794	3776	3669.1	598.1	<0.001
	Senergy	92	287.9	2591	902.9	963.3	425.5	42	189.2	1525.2	641.5	673	282.2	<0.001
	PLenergy	92	233.8	991.9	471.4	496	139.8	42	172.5	1275.1	449.3	483.5	176.4	0.686
	Penergy	92	189.9	788.5	406.4	423.1	137.3	42	218.3	609.7	408.3	420.3	97.7	0.890
	Lenergy	92	89.6	944.2	477.2	475.1	161.8	42	123.8	899.6	440.2	452.2	174.1	0.474
Female	AGE	143	67	92	79	79.2	5.7	68	67	93	79.5	79.7	6.1	0.544
	HEIGHT	143	139.2	172.9	159.5	159.3	5.6	68	145.1	173.4	159.5	159.3	6.1	0.995
	WEIGHT	143	37.2	112	66.4	68.7	13.7	68	39.2	111.2	63.4	64.2	15	0.036
	PLy	143	314	3071	987	1093.3	476.5	68	353	1945	780	850	336	<0.001
	PLu	143	1816	4535	2837	2963.9	551.2	68	1700	4419	2632	2693.3	440	<0.001
	Sy	143	1272	9446	2924	3362.6	1543.1	68	1300	5913	2528	2680.2	891.6	<0.001
	Su	143	3611	16330	6775	7256.1	2335.8	68	3085	10675	5831.5	6045.3	1609.2	<0.001
	Py	143	525	2733	1154	1247.8	468.9	68	490	2049	928	1006.9	341.6	<0.001
	Pu	143	1933	3893	2539	2641.6	399.4	68	1610	3150	2373	2425.3	349	<0.001
	Ly	143	469	3736	1319	1432.2	585.8	68	570	2532	1004	1074.5	382	<0.001
	Lu	143	1941	5386	3203	3256.7	650.6	68	1945	4896	2989.5	3019.9	551.4	0.007
	Senergy	143	195.2	1770.3	492.6	558.4	275.8	68	196.5	1115.5	396.7	423.3	155.1	<0.001
	PLenergy	143	56.1	800.1	403.6	414.6	125.3	68	118.6	912.6	393.2	412.1	139	0.899
	Penergy	143	84.9	787.1	362.9	377	118.9	68	158.1	606.2	360.8	367	96.5	0.513
	Lenergy	143	86.1	943.7	385.8	390.9	154.3	68	119.2	775.4	384.5	382.8	147	0.714

Table 2. The abbreviations of FE parameters.

FE Parameters	Stance	Loading Condition		
		Posterior	Posterolateral	Lateral
Yield strength (force at onset of fracture)	Sy	Py	PLy	Ly
Ultimate strength (load capacity)	Su	Pu	PLu	Lu
Energy to failure	Senergy	Penergy	PLenergy	Lenergy

Table 3. Multiple linear regression results for each of the 12 FE parameters for all subjects, including coefficients of standardized variables, standard errors, and *p*-values in italics.

Dependent variable	Regression coefficients for standardized variables (Standard error)								<i>R</i> ²
	<i>p</i>		FX	Sex	Age	Weight	Height	Fx:Age	Fx:Sex
	FX	Sex	Age	Weight	Height	Fx:Age	Fx:Sex	Fx:Height	
PLy	-0.301 (0.115) <i>0.009</i>	0.706 (0.158) <i><0.001</i>	-0.147 (0.055) <i>0.007</i>	0.298 (0.056) <i><0.001</i>	0.033 (0.107) 0.759		-0.420 (0.183) <i>0.022</i>		0.3773
	-0.299 (0.101) <i>0.003</i>	0.833 (0.138) <i><0.001</i>	-0.151 (0.040) <i><0.001</i>	0.294 (0.047) <i><0.001</i>	0.130 (0.072) <i>0.072</i>		-0.400 (0.160) <i>0.013</i>		0.5467
	-0.290 (0.148) <i>0.050</i>	0.607 (0.179) <i>0.001</i>	-0.244 (0.069) <i><0.001</i>	0.237 (0.057) <i><0.001</i>	0.097 (0.124) 0.435	0.144 (0.115) 0.212	-0.491 (0.320) 0.127	0.028 (0.209) 0.892	0.3571
PLu	-0.315 (0.105) <i>0.003</i>	0.651 (0.144) <i><0.001</i>	-0.183 (0.050) <i><0.001</i>	0.327 (0.050) <i><0.001</i>	0.146 (0.075) <i>0.052</i>	0.121 (0.080) 0.134	-0.500 (0.167) <i>0.003</i>		0.511
	-0.325 (0.115) <i>0.005</i>	0.696 (0.159) <i><0.001</i>	-0.268 (0.067) <i><0.001</i>	0.248 (0.057) <i><0.001</i>	0.060 (0.107) 0.576	0.165 (0.106) 0.121	-0.493 (0.184) <i>0.008</i>		0.3806
	-0.124 (0.137) 0.366	0.941 (0.159) <i><0.001</i>	-0.151 (0.051) <i>0.003</i>	0.243 (0.049) <i><0.001</i>	0.077 (0.085) 0.364	0.234 (0.086) <i>0.007</i>	-0.800 (0.287) <i>0.006</i>	0.332 (0.143) <i>0.021</i>	0.5217
Sy	-0.417 (0.111) <i><0.001</i>	0.713 (0.153) <i><0.001</i>	-0.295 (0.064) <i><0.001</i>	0.234 (0.054) <i><0.001</i>	0.069 (0.103) 0.505	0.187 (0.102) <i>0.069</i>	-0.437 (0.177) <i>0.014</i>		0.4201
	-0.201 (0.104) <i>0.054</i>	0.780 (0.142) <i><0.001</i>	-0.183 (0.050) <i><0.001</i>	0.266 (0.049) <i><0.001</i>	0.180 (0.074) <i>0.015</i>	0.125 (0.079) 0.117	-0.492 (0.165) <i>0.003</i>		0.521
	-0.299 (0.140) <i>0.034</i>	0.593 (0.170) <i>0.001</i>	-0.168 (0.066) <i>0.011</i>	0.288 (0.054) <i><0.001</i>	0.203 (0.118) <i>0.085</i>	0.121 (0.110) 0.274	-0.360 (0.305) 0.239	-0.053 (0.199) 0.789	0.4343
Fenergy		0.112 (0.160) 0.485		0.111 (0.064) <i>0.082</i>	0.247 (0.117) <i>0.035</i>				0.109
	-0.089 (0.111) <i>0.424</i>	0.047 (0.181) 0.797	0.075 (0.082) 0.359	-0.007 (0.069) 0.918	0.274 (0.131) <i>0.037</i>	0.205 (0.130) 0.116			0.0677
		-0.190 (0.178) <i>0.286</i>	-0.096 (0.066) <i>0.144</i>	0.121 (0.067) <i>0.072</i>	0.157 (0.128) 0.221				0.0991

Notes: The bold-faced value means the variable is not significant (*p*>0.1). “-” indicates that the variable was not included in the model because the *p*-values would have been greater than 0.1.

Table 4. The average AUCs of the classification models using stratified leave-one-group-out cross-validation for the fracture status prediction using only the covariates, the PC1 plus the covariates, and the nine FE parameters combined plus the covariates, respectively.

Model	Sample	Average AUC (Standard error)		
		Only Covariates	PC1 + Covariates	FE parameters combined + Covariates
Logistic	All	0.699 (0.052)	0.738 (0.043)	0.724 (0.041)
	Male	0.727 (0.093)	0.777 (0.093)	0.745 (0.094)
	Female	0.608 (0.115)	0.623 (0.095)	0.669 (0.089)
LDA	All	0.696 (0.053)	0.725 (0.046)	0.708 (0.044)
	Male	0.727 (0.090)	0.758 (0.099)	0.751 (0.105)
	Female	0.608 (0.116)	0.615 (0.110)	0.659 (0.080)
PLS	All	0.700 (0.049)	0.737 (0.045)	0.731 (0.049)
	Male	0.719 (0.093)	0.788 (0.113)	0.753 (0.117)
	Female	0.617 (0.068)	0.638 (0.087)	0.611 (0.086)
RF	All	0.640 (0.045)	0.684 (0.042)	0.727 (0.049)
	Male	0.714 (0.107)	0.745 (0.086)	0.742 (0.072)
	Female	0.555 (0.060)	0.577 (0.075)	0.569 (0.075)
QDA	All	0.637 (0.073)	0.695 (0.056)	0.681 (0.052)
	Male	0.690 (0.110)	0.707 (0.141)	0.674 (0.101)
	Female	0.584 (0.085)	0.622 (0.067)	0.649 (0.083)
MDA	All	0.668 (0.056)	0.702 (0.047)	0.661 (0.048)
	Male	0.724 (0.078)	0.719 (0.105)	0.664 (0.102)
	Female	0.585 (0.074)	0.632 (0.066)	0.645 (0.064)
NNET	All	0.693 (0.061)	0.731 (0.050)	0.719 (0.046)
	Male	0.699 (0.109)	0.744 (0.110)	0.714 (0.093)
	Female	0.632 (0.115)	0.563 (0.136)	0.622 (0.099)
MARS	All	0.668 (0.052)	0.717 (0.039)	0.689 (0.054)
	Male	0.573 (0.127)	0.724 (0.115)	0.664 (0.137)
	Female	0.585 (0.086)	0.558 (0.094)	0.667 (0.085)
KNN	All	0.607 (0.120)	0.689 (0.074)	0.691 (0.065)
	Male	0.671 (0.128)	0.744 (0.096)	0.681 (0.128)
	Female	0.511 (0.078)	0.517 (0.109)	0.554 (0.104)

Notes: The bold-faced value means the largest AUCs among three comparison models.

Figure 1. The correlation coefficients among 12 FE parameters for all subjects.

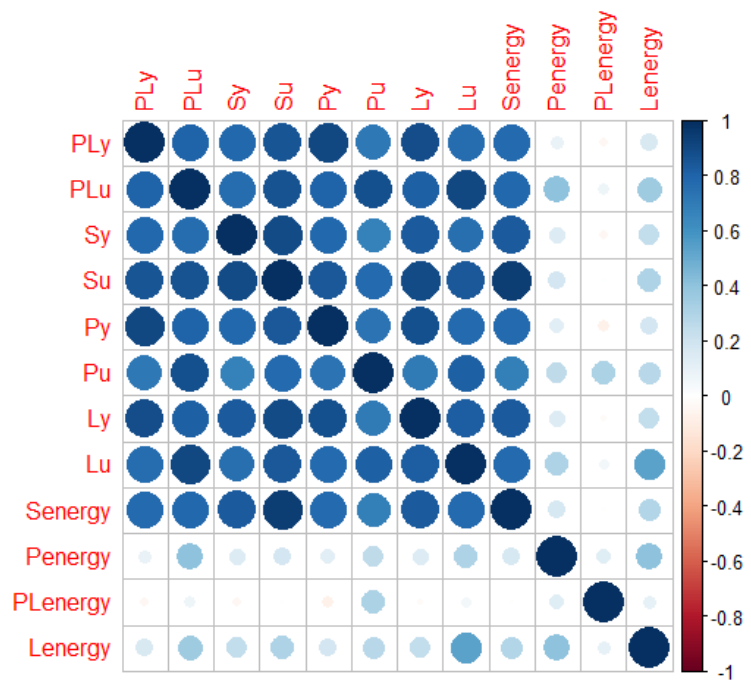


Figure 2. The predictive performance of Logistic and PLS based on stratified resampling. The values over the lines indicated the *p* values were obtained from the one-sided Student's t-test. The values in the boxes indicated the average AUCs by using the 1st PC along with the covariates (PC1 + Cov) versus using covariates only (Cov) or FE parameters combined along with covariates (FE combined + Cov).

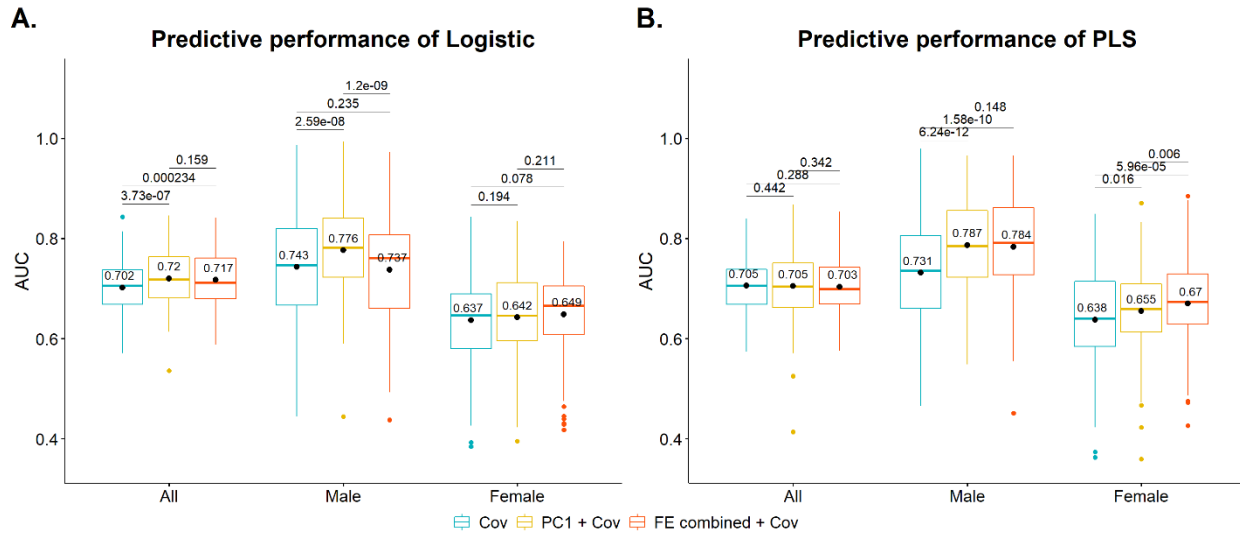


Figure 3. The predictive performance of PLS for each FE parameters compared with that for the 1st PC. The values over the lines indicated the *p* values were obtained from the one-sided Student's t-test. The values in the boxes indicated the average AUCs by using the 1st PC along with the covariates (PC1 + Cov) versus using each of FE parameters along with covariates (* + Cov).

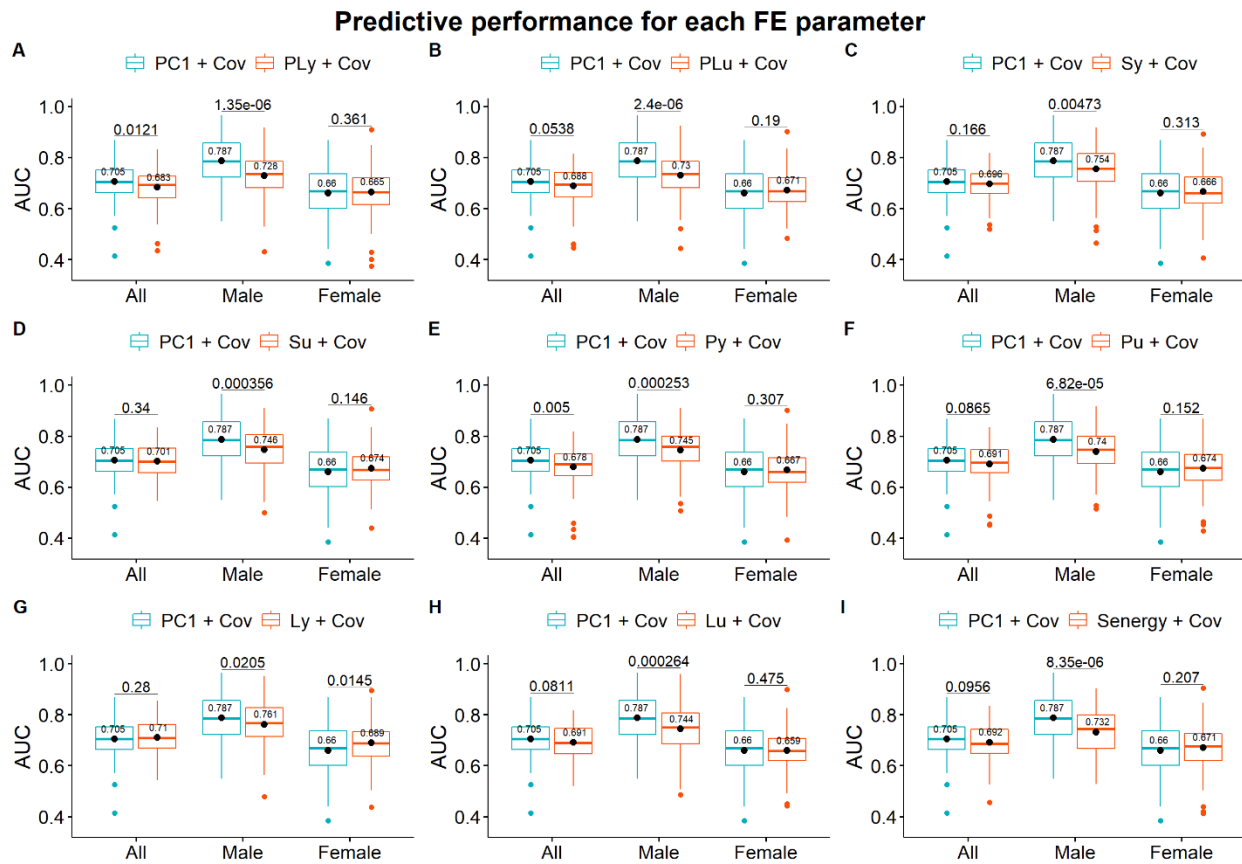
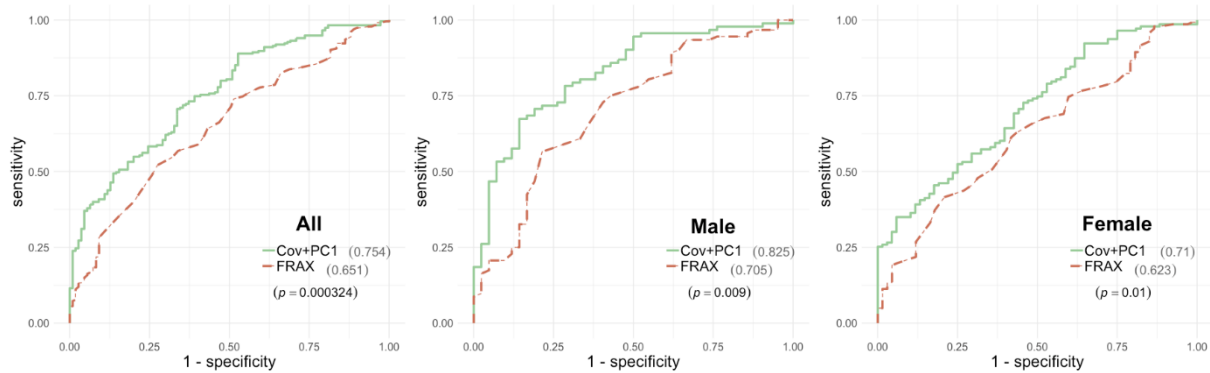


Figure 4. The performance of the hip fracture prediction for PC1 and FRAX for the all sample (left), male sample (middle), and female sample (right).



Reference

1. Richards, J.B., H.-F. Zheng, and T.D. Spector, *Genetics of osteoporosis from genome-wide association studies: advances and challenges*. Nature Reviews Genetics, 2012. **13**(8): p. 576-588.
2. Melton III, L.J., *Adverse outcomes of osteoporotic fractures in the general population*. Journal of Bone and Mineral Research, 2003. **18**(6): p. 1139-1141.
3. Melton, L.J., *The prevalence of osteoporosis: gender and racial comparison*. Calcified tissue international, 2001. **69**(4): p. 179.
4. Zhao, L.J., et al., *Correlation of obesity and osteoporosis: effect of fat mass on the determination of osteoporosis*. Journal of bone and mineral research, 2008. **23**(1): p. 17-29.
5. Recker, R. and D. Kimmel, *Changes in trabecular microstructure in osteoporosis occur with normal bone remodeling dynamics*. J Bone Miner Res, 1991. **6**(S1): p. S225.
6. Yang, T.-L., et al., *Genome-wide copy-number-variation study identified a susceptibility gene, UGT2B17, for osteoporosis*. The American Journal of Human Genetics, 2008. **83**(6): p. 663-674.
7. Yang, T.-L., et al., *A road map for understanding molecular and genetic determinants of osteoporosis*. Nature Reviews Endocrinology, 2020. **16**(2): p. 91-103.
8. Keyak, J., et al., *Effect of finite element model loading condition on fracture risk assessment in men and women: the AGES-Reykjavik study*. Bone, 2013. **57**(1): p. 18-29.
9. Wright, N.C., et al., *The recent prevalence of osteoporosis and low bone mass in the United States based on bone mineral density at the femoral neck or lumbar spine*. Journal of Bone and Mineral Research, 2014. **29**(11): p. 2520-2526.
10. Fogel, H.A. and L.G. Jenis, *The Economic Burden of Osteoporosis*, in *Vertebral Compression Fractures in Osteoporotic and Pathologic Bone*. 2020, Springer. p. 21-29.
11. Melton, L.r., et al., *Secular trends in hip fracture incidence and recurrence*. Osteoporosis International, 2009. **20**(5): p. 687-694.

12. Keene, G.S., M.J. Parker, and G.A. Pryor, *Mortality and morbidity after hip fractures*. British medical journal, 1993. **307**(6914): p. 1248-1250.
13. Cooper, C., et al., *Population-based study of survival after osteoporotic fractures*. American journal of epidemiology, 1993. **137**(9): p. 1001-1005.
14. Leibson, C.L., et al., *Mortality, disability, and nursing home use for persons with and without hip fracture: a population-based study*. Journal of the American Geriatrics Society, 2002. **50**(10): p. 1644-1650.
15. Magaziner, J., et al., *Excess mortality attributable to hip fracture in white women aged 70 years and older*. American journal of public health, 1997. **87**(10): p. 1630-1636.
16. Magaziner, J., et al., *Predictors of functional recovery one year following hospital discharge for hip fracture: a prospective study*. Journal of gerontology, 1990. **45**(3): p. M101-M107.
17. Kannus, P., et al., *Epidemiology of osteoporotic ankle fractures in elderly persons in Finland*. Annals of internal medicine, 1996. **125**(12): p. 975-978.
18. Riggs, B.L. and L. Melton lii, *The worldwide problem of osteoporosis: insights afforded by epidemiology*. Bone, 1995. **17**(5): p. S505-S511.
19. Ammann, P. and R. Rizzoli, *Bone strength and its determinants*. Osteoporosis international, 2003. **14**(3): p. 13-18.
20. Blake, G.M. and I. Fogelman, *The role of DXA bone density scans in the diagnosis and treatment of osteoporosis*. Postgraduate medical journal, 2007. **83**(982): p. 509-517.
21. Genant, H., K. Engelke, and S. Prevrhal, *Advanced CT bone imaging in osteoporosis*. Rheumatology, 2008. **47**(suppl_4): p. iv9-iv16.
22. Kanis, J.A., *Assessment of fracture risk and its application to screening for postmenopausal osteoporosis: synopsis of a WHO report*. Osteoporosis international, 1994. **4**(6): p. 368-381.
23. Rosen, C.J., *Primer on the metabolic bone diseases and disorders of mineral metabolism*. 2009: John Wiley & Sons.

24. Marshall, D., O. Johnell, and H. Wedel, *Meta-analysis of how well measures of bone mineral density predict occurrence of osteoporotic fractures*. *Bmj*, 1996. **312**(7041): p. 1254-1259.
25. Chang, G., et al., *Finite element analysis applied to 3-T MR imaging of proximal femur microarchitecture: lower bone strength in patients with fragility fractures compared with control subjects*. *Radiology*, 2014. **272**(2): p. 464-474.
26. Carballido-Gamio, J., et al., *Automatic multi-parametric quantification of the proximal femur with quantitative computed tomography*. *Quantitative imaging in medicine and surgery*, 2015. **5**(4): p. 552.
27. Keyak, J., et al., *Male–female differences in the association between incident hip fracture and proximal femoral strength: a finite element analysis study*. *Bone*, 2011. **48**(6): p. 1239-1245.
28. Orwoll, E.S., et al., *Finite element analysis of the proximal femur and hip fracture risk in older men*. *Journal of bone and mineral research*, 2009. **24**(3): p. 475-483.
29. Jolliffe IT, Cadima J. *Principal component analysis: a review and recent developments*. *Philosophical Transactions of the Royal Society A: Mathematical, Physical and Engineering Sciences*. 2016 Apr 13;374(2065):20150202.
30. Sarker IH. *Machine learning: Algorithms, real-world applications and research directions*. *SN Computer Science*. 2021 May;2(3):1-21.
31. Harris, T.B., et al., *Age, gene/environment susceptibility–Reykjavik Study: multidisciplinary applied phenomics*. *American journal of epidemiology*, 2007. **165**(9): p. 1076-1087.
32. Keyak, J., et al., *Hip load capacity and yield load in men and women of all ages*. *Bone*. 2020 Aug;137:115321.
33. Keyak, J., et al., *Prediction of femoral fracture load using automated finite element modeling*. *J Biomech*. 1998; 31:125–133.
34. Keyak, J., et al., *Improved prediction of proximal femoral fracture load using nonlinear finite element models*. *Med Eng Phys*. 2001; 23:165–173.
35. Keyak, J., et al., *Predicting proximal femoral strength using structural engineering models*. *Clinl Orthop Relat Res*. 2005; 437:219–228.

36. Keyak, J., et al., *Reduction in proximal femoral strength due to long-duration spaceflight*. Bone. 2009; 44:449–453
37. Kuhn, M. and K. Johnson, *Applied predictive modeling*. Vol. 26. 2013: Springer.
38. Kanis, J. A., et al. *FRAX™ and the assessment of fracture probability in men and women from the UK*. Osteoporosis international, 2008. 19.4: 385-397.
39. Cody D.D., et al. *Femoral strength is better predicted by finite element models than QCT and DXA*. J Biomech. 1999; 32:1013–1020.
40. Closkey E.V., et al. *A meta-analysis of trabecular bone score in fracture risk prediction and its relationship to FRAX*. J Bone Miner Res 2016; 31: 940–948.
41. Kanis J.A., et al. *Interpretation and use of FRAX in clinical practice*. Osteoporos Int 2011; 22: 2395–2411.